True Direction Equilibrium Flux Method applications on rectangular 2D meshes

Mechanical Engineering Report No. 2006/06

M.R. Smith, M.N. Macrossan

Centre for Hypersonics, The University of Queensland

Brisbane, 4072, Australia

M. V. Metchnik and P. A. Pinto

Steward Observatory, University of Arizona

933 N Cherry Av, Tucson, AZ 85722-0065, USA

June 8, 2006

Abstract

In a finite volume CFD method for unsteady flow fluxes of mass, momentum and energy are exchanged between cells over a series of small time steps. The conventional approach, which we will refer to as *direction decoupling*, is to estimate fluxes across interfaces in a regular array of cells by using a one-dimensional flux expression based on the component of flow velocity normal to the interface. This means that fluxes cannot be exchanged between diagonally adjacent cells since they share no cell interface, even if the local flow conditions dictate that the fluxes should flow diagonally. The direction decoupling imposed by the numerical method requires that the fluxes reach a diagonally adjacent cell in two time-steps.

Here we present a *true direction flux method*, which is an updated version of Pullin's Equilibrium Flux Method (EFM) [1] in which fluxes are derived from kinetic theory. Previous implementations of EFM in higher dimensions ([2], [3], [4]) have used direction decoupling as described above. In this *True Direction Equilibrium Flux Method* (TDEFM) fluxes flow not only between cells sharing an interface, but also to diagonally connecting cells, or ultimately to any cell in the grid. We compare TDEFM results to those from a direction-decoupled methods using 1D fluxes calculated with EFM and a Godunove solver. The test flow is a cylindrically symmetric implosion which we solve on a two-dimensional Cartesian grid, with cell interfaces parallel to the x and y axes. Because the flow is in theory radially symmetric, any lack of radial symmetry in the solution can be used to assess the inaccuracies in the computed results. The conventional direction decoupling methods with 1D solver flux calculations (EFM or Godunov Method) produced greater asymmetries (inaccuracies) in the solution than did the new method.

TDEFM requires 1% less CPU time than the direction decoupled Riemann solver and 15% more CPU time than direction decoupled EFM.

1 Introduction

Bird's Direct Simulation Monte-Carlo method simulates a rarefied flow by following the motion and collisions of a large number of simulator particles as they move through the flow. DSMC in the high collision rate limit has been used as an Euler solver ([1],[5]) and as the 'continuum' part of a hybrid DSMC/continuum solver. DSMC is generally more robust than a conventional Euler solver but suffers from statistical scatter which requires large amounts of CPU power to reduce to acceptable limits. One reason for DSMC's stability is that the fluxes of mass, momentum and energy are carried by particles which move in the physically correct directions; in any time step fluxes may flow from any cell to any other cell in the computational domain. In continuum solvers the fluxes are *direction decoupled*: one dimensional flux calculations are performed in the direction normal to the interface between two cells, and the fluxes are exchanged with adjacent cells only. For example, on a 2D structured grid the fluxes flow in two coordinate directions and never flow in one time step between cells which are diagonally contiguous (share a vertex in common) but do not have a common interface. Cook [6] shows that when the cell structure is not well aligned with the physical structures in the flow, 'direction-decoupled' methods may produce unphysical results such as negative temperatures or densities where strong shocks occur or interact. These solvers may also produce asymmetrical results where symmetrical results are theoretically expected or required.

Macrossan *et al.* [7] used the 'Particle Flux Method' to mimic the effect of high-collision rate limit DSMC, but cut down greatly on computational effort. Some statistical scatter was unavoidable, since particles, which were generated statistically within each cell, were used to carry the fluxes to other cells. Pullin [1] proposed the Equilibrium Flux Method (EFM) in which the fluxes carried by particles having velocities conforming to the local Maxwell-Boltzmann distribution were calculated analytically for the limit of an infinite number of particles. EFM eliminates the statistical scatter associated with the effectively equivalent particle flux methods. When EFM was used in 2D and 3D flows ([2], [3],[8]) the conventional direction decoupling approach described above was used.

Since the EFM fluxes are just the amounts of mass, momentum and energy transported by molecules in free-molecular flight there is no need, other than for simplicity, to use direction decoupling when EFM is applied in two or three dimensions. Metchnik and Pinto (personal communication) have derived reasonably simple expressions for the fluxes carried by molecules, originating in a rectangular cell with velocities selected from the Maxwell-Boltzmann distribution, and moving in a specified time of flight to any other rectangular region. This method, which we called TDEFM, or True Direction Equilibrium Flux Method, is derived from kinetic theory. The fluxes calculated in this method are exchanged between all cells in the region. Mass, energy and momentum are all perfectly conserved. Direction decoupling is not necessary since analytical expressions for the fluxes carried by particles between any two cells in a Cartesian grid have been used. TDEFM is the analytical form of the infinite collision limit of DSMC and allows fluxes to be exchanged between non-adjacent cells. TDEFM has none of the statistical scatter associated with the particle nature of DSMC. The TDEFM flux calculations used in this report are restricted to 1st order in space. Results are shown along with those from traditional EFM and an approximate Riemann solver [9].

2 TDEFM

Derived below are the expressions for the mass, momentum and energy carried by molecules in free-molecular flight for time Δt, starting from a rectangular region (in 2D) to any other rectangular region. For simplicity all forces acting on particles are assumed to be zero, *i.e.* no particle interactions occur while particles are moving. Internal energy is included in the energy flux expressions[1] so monoatomic, diatomic or polyatomic gases can be simulated.

Uniform conditions are assumed within the cell from which the molecules originate (*i.e.* there are no gradients of density, mean velocity or temperature within the cell) and all the molecules within the cell have velocities conforming to the same Maxwell-Boltzmann distribution. The distribution function for components of molecular velocity, $v_j \equiv v_x$ or v_y or v_z, has the Maxwell-Boltzmann form

$$f\left(v_x, v_y, v_z\right) = g\left(v_x\right) g\left(v_y\right) g\left(v_z\right)$$

where

$$g\left(v_j\right) = \frac{1}{\pi^{1/2} c_m} \exp\left[-\frac{\left(v_j - V_j\right)^2}{c_m^2}\right],\ V_j \equiv \bar{v}_j = \int_{-\infty}^{\infty} v_j g dv_j \text{ and } c_m = \left(2RT\right)^{-1/2}.$$

In other words, the fraction of molecules having a velocity v_x in the range $v_x \rightarrow v_x + dv_x$ is $g\left(v_x\right) dv_x$ and similar expressions hold for v_y and v_z. The components of the mean flow velocity (mean molecular velocity) in any cell are V_x and V_y (and $V_z = 0$ for 2D flow), the mass density is $\rho = m_p n$, where m_p is the mass of one molecule and n is the number density (molecules/m^3). The random thermal velocity is $c_j = v_j - V_j$ and the three components of translational kinetic temperature are given by $RT_j = \int_{-\infty}^{\infty} c_j^2\, dv_j$ where R is the ordinary gas constant. All kinetic temperatures are the same and the 'overall' kinetic temperature is $T = \left(T_x + T_y + T_z\right)/3 = T_x = T_y = T_z$. The most probable thermal speed is $c_m = \left(2RT\right)^{1/2}$.

Setting $s \equiv \sqrt{RT}$ and $m \equiv V_j$ the expression for $g(v)$ can be rewritten as:

$$g(v_j) = \frac{1}{\sqrt{2\pi} s} \exp\left(\frac{-(v_j - m)^2}{2s^2}\right) \tag{1}$$

The probability of a particle with a velocity between a and b, or P_m, is:

$$P_m = \int_a^b \frac{1}{\sqrt{2\pi} s} \exp\left(\frac{-(v_j - m)^2}{2s^2}\right) dv_j \tag{2}$$

The general solution to this integral is:

$$\int \frac{1}{\sqrt{2\pi} s} \exp \frac{-(v_j - m)^2}{2s^2} dv_j = \frac{1}{2} s.\mathrm{erf}\left(\frac{m - v_j}{\sqrt{2} s}\right) \tag{3}$$

[1]Internal here means 'internal' to the molecule, and is different from the internal energy of classical thermodynamics, which of course includes the random translational energy of the molecules. Hence we prefer to use the term 'structure' energy to denote the energy stored by virtue of the structure of the molecule.

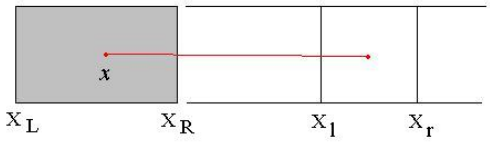

Figure 1: Particle moving from x (between x_L and x_R) to a region between x_l and x_r. For the derivations used here, $x_r \geq x_l$ & $x_R \geq x_L$

Referring to Figure 1, for a particle at location x to travel to a location between x_l and x_r in a time space t, the velocity range falls between $\frac{x-x_l}{t}$ and $\frac{x-x_r}{t}$. Therefore, we can reevaluate the integral in Equation 2 to obtain:

$$P_m = \int_{\left(\frac{x-x_l}{t}\right)}^{\left(\frac{x-x_r}{t}\right)} \frac{1}{\sqrt{2\pi}s} \exp \frac{-(v_x - m)^2}{2s^2} dv_x \tag{4}$$

Evaluating the bounds of this integral and using the result from Equation 3 we obtain:

$$P_m = -\frac{1}{2}\left[\text{erf}\left(\frac{m - \frac{x_r - x}{t}}{\sqrt{2}s}\right) - \text{erf}\left(\frac{m - \frac{x_l - x}{t}}{\sqrt{2}s}\right)\right] \tag{5}$$

or:

$$P_m = \frac{1}{2}\left[\text{erf}\left(\frac{mt + x - x_l}{\sqrt{2}st}\right) - \text{erf}\left(\frac{mt + x - x_r}{\sqrt{2}st}\right)\right] \tag{6}$$

The cumulative probability of a particle having the required velocity range between x_L and x_R we will call f_{ME}. This also represents the fraction of particles from the region between x_L and x_R possessing the velocities specified. This is evaluated as:

$$f_{ME} = \int_{x_L}^{x_R} P_m dx \tag{7}$$

or:

$$f_{ME} = \int_{x_L}^{x_R} \frac{1}{2}\left[\text{erf}\left(\frac{mt + x - x_l}{\sqrt{2}st}\right) - \text{erf}\left(\frac{mt + x - x_r}{\sqrt{2}st}\right)\right] dx \tag{8}$$

To find the total flux flowing across the surface at x_R, the integral of P_m needs to be evaluated using $x_l = X_R$ and $x_r = \infty$. Thus:

$$P_m = \frac{1}{2}\left[\text{erf}\left(\frac{mt + x - x_R}{\sqrt{2}st}\right) - \text{erf}\left(\frac{mt + x - \infty}{\sqrt{2}st}\right)\right] \tag{9}$$

Simplifying this obtains:

$$P_m = \frac{1}{2}\left[\text{erf}\left(\frac{mt + x - x_R}{\sqrt{2}st}\right) - 1\right] \tag{10}$$

This needs to be substituted into Equation 8. The general solution to this integral is:

$$\int P_m dx = \frac{st}{\sqrt{2\pi}} \exp\left(\frac{-\left(mt - x_R + x\right)^2}{2s^2t^2}\right) - \frac{x}{2} + \frac{1}{2}\left(mt - x_R + x\right) \text{erf}\left(\frac{mt - x_R + x}{\sqrt{2}st}\right) \tag{11}$$

Using bounds x_L and x_R, this evaluates to:

$$\begin{aligned} f_{ME} &= \textstyle\int_{x_L}^{x_R} P_a dx = \frac{st}{\sqrt{2\pi}} \exp\left(-\frac{m^2}{2s^2}\right) - \frac{st}{\sqrt{2\pi}} \exp\left(\frac{-(mt-x_R+x_L)^2}{2s^2t^2}\right) \\ &+\tfrac{1}{2}(x_R - x_L) + \tfrac{1}{2}(mt)\operatorname{erf}\left(\frac{m}{\sqrt{2}s}\right) - \tfrac{1}{2}(mt - x_R + x_L)\operatorname{erf}\left(\frac{mt-x_R+x_L}{\sqrt{2}st}\right) \end{aligned} \tag{12}$$

This is equivalent to the flux flowing through the surface at x_R and should be equal to the EFM flux. By integrating P_m and setting x_r to a finite value rather than ∞ (and keeping $x_l = x_R$), we can find the fraction of mass that flows from between x_L and x_R into an immediately adjacent region. Thus, P_m can be re-evaluated as:

$$P_m = \frac{1}{2}\left[\operatorname{erf}\left(\frac{mt + x - x_R}{\sqrt{2}st}\right) - \operatorname{erf}\left(\frac{mt + x - x_r}{\sqrt{2}st}\right)\right] \tag{13}$$

The general solution to this integral is:

$$\begin{aligned} &\textstyle\int P_m dx = \\ &\tfrac{st}{\sqrt{2\pi}}\left[\exp\left(\tfrac{-(mt+x-x_R)^2}{2s^2t^2}\right) - \exp\left(\tfrac{-(mt+x-x_r)^2}{2s^2t^2}\right)\right] \\ &+\tfrac{1}{2}(mt + x - x_R)\operatorname{erf}\left(\tfrac{mt+x-x_R}{\sqrt{2}st}\right) \\ &-\tfrac{1}{2}(mt + x - x_r)\operatorname{erf}\left(\tfrac{mt+x-x_r}{\sqrt{2}st}\right) \end{aligned} \tag{14}$$

Evaluating this integral over the bounds x_L and x_R obtains:

$$\begin{aligned} &\textstyle\int_{x_L}^{x_R} P_m dx = \tfrac{st}{\sqrt{2\pi}}\left[\exp\left(\tfrac{-m^2}{2s^2}\right) - \exp\left(\tfrac{-(mt+x_L-x_R)^2}{2s^2t^2}\right) - \exp\left(\tfrac{-(mt+x_R-x_r)^2}{2s^2t^2}\right) + -\exp\left(\tfrac{-(mt+x_L-x_r)^2}{2s^2t^2}\right)\right] \\ &+\tfrac{1}{2}(mt)\operatorname{erf}\left(\tfrac{m}{\sqrt{2}s}\right) - \tfrac{1}{2}(mt + x_L - x_R)\operatorname{erf}\left(\tfrac{mt+x_L-x_R}{\sqrt{2}st}\right) \\ &-\tfrac{1}{2}(mt + x_R - x_r)\operatorname{erf}\left(\tfrac{mt+x_R-x_r}{\sqrt{2}st}\right) + \tfrac{1}{2}(mt + x_L - x_r)\operatorname{erf}\left(\tfrac{mt+x_L-x_r}{\sqrt{2}st}\right) \end{aligned} \tag{15}$$

If $x_l \neq x_R$ but instead was any value $x_l >= x_R$, the general expression for fraction of mass flow to any region $x_l - x_r$ from $x_L - x_R$ would be:

$$\begin{aligned} &f_{ME} = \tfrac{st}{\sqrt{2\pi}} \\ &\left[\exp\left(\tfrac{-(mt+x_R-x_l)^2}{2s^2t^2}\right) - \exp\left(\tfrac{-(mt+x_L-x_l)^2}{2s^2t^2}\right) - \exp\left(\tfrac{-(mt+x_R-x_r)^2}{2s^2t^2}\right) + -\exp\left(\tfrac{-(mt+x_L-x_r)^2}{2s^2t^2}\right)\right] \\ &-\tfrac{1}{2}(mt + x_R - x_l)\operatorname{erf}\left(\tfrac{mt+x_R-x_l}{\sqrt{2}st}\right) - \tfrac{1}{2}(mt + x_L - x_l)\operatorname{erf}\left(\tfrac{mt+x_L-x_l}{\sqrt{2}st}\right) \\ &-\tfrac{1}{2}(mt + x_R - x_r)\operatorname{erf}\left(\tfrac{mt+x_R-x_r}{\sqrt{2}st}\right) + \tfrac{1}{2}(mt + x_L - x_r)\operatorname{erf}\left(\tfrac{mt+x_L-x_r}{\sqrt{2}st}\right) \end{aligned} \tag{16}$$

A simple substitution of $x_l = x_R$ in Equation 16 gives the same result as Equation 15. This equation can be used to find the faction of mass from region $x_L \leftrightarrow x_R$ that flows into the region between $x_l \leftrightarrow x_r$.

The mean velocity of particles (or the mean momentum per unit mass) from location x to land in the region between x_l and x_r is defined as:

$$P_p = \int_{\frac{x_l - x}{\Delta t}}^{\frac{x_r - x}{\Delta t}} v_x \frac{1}{\sqrt{2\pi s}} \exp\left(\frac{-(v_x - m)^2}{2s^2}\right) dv_x \tag{17}$$

The general solution to this integral is:

$$P_p = \left[-\frac{s}{\sqrt{2\pi}} \exp\left(\frac{-(m - v_x)^2}{2s^2}\right) - \frac{m}{2} \text{erf}\left(\frac{m - v_x}{\sqrt{2}s}\right) \right]_{\frac{x_l - x}{\Delta t}}^{\frac{x_r - x}{\Delta t}} \tag{18}$$

Substituting bounds and rearranging terms obtains:

$$\begin{aligned} P_p = {} & \tfrac{s}{\sqrt{2\pi}} \left[\exp\left(\tfrac{-(mt+x-x_l)^2}{2s^2t^2}\right) - \exp\left(\tfrac{-(mt+x-x_r)^2}{2s^2t^2}\right) \right] \\ & + \tfrac{m}{2} \left[\text{erf}\left(\tfrac{mt+x-x_l}{\sqrt{2}st}\right) - \text{erf}\left(\tfrac{mt+x-x_r}{\sqrt{2}st}\right) \right] \end{aligned} \tag{19}$$

The cumulative average velocity of particles moving into region $x_l \leftrightarrow x_r$ from region $x_L \leftrightarrow x_R$ is:

$$f_{PE} = \int_{x_L}^{x_R} P_p dx \tag{20}$$

The general solution to this integral is:

$$\begin{aligned} f_{PE} = \int P_p dx = {} & \tfrac{mst}{\sqrt{2\pi}} \left[\exp\left(\tfrac{-(mt+x-x_l)^2}{2s^2t^2}\right) - \exp\left(\tfrac{-(mt+x-x_r)^2}{2s^2t^2}\right) \right] \\ & + \left(\tfrac{1}{2}\right) (m(mt + x - x_l) + s^2 t) \, \text{erf}\left(\tfrac{mt+x-x_l}{\sqrt{2}st}\right) \\ & + \left(\tfrac{1}{2}\right) (m(mt + x - x_r) + s^2 t) \, \text{erf}\left(\tfrac{mt+x-x_r}{\sqrt{2}st}\right) \end{aligned} \tag{21}$$

Evaluating from x_L to x_R gives:

$$
\begin{aligned}
&f_{PE} = \tfrac{mst}{\sqrt{2\pi}} \\
&\left[\exp\left(\tfrac{-(mt+x_R-x_l)^2}{2s^2t^2}\right) - \exp\left(\tfrac{-(mt+x_L-x_l)^2}{2s^2t^2}\right) - \exp\left(\tfrac{-(mt+x_R-x_r)^2}{2s^2t^2}\right) + -\exp\left(\tfrac{-(mt+x_L-x_r)^2}{2s^2t^2}\right)\right] \\
&-\left(\tfrac{1}{2}\right)(m(mt+x_R-x_l)+s^2t)\operatorname{erf}\left(\tfrac{mt+x_R-x_l}{\sqrt{2}st}\right) - \left(\tfrac{1}{2}\right)(m(mt+x_L-x_l)+s^2t)\operatorname{erf}\left(\tfrac{mt+x_L-x_l}{\sqrt{2}st}\right) \\
&-\left(\tfrac{1}{2}\right)(m(mt+x_R-x_r)+s^2t)\operatorname{erf}\left(\tfrac{mt+x_R-x_r}{\sqrt{2}st}\right) + \left(\tfrac{1}{2}\right)(m(mt+x_L-x_r)+s^2t)\operatorname{erf}\left(\tfrac{mt+x_L-x_r}{\sqrt{2}st}\right)
\end{aligned}
\tag{22}
$$

The mean energy of particles (per unit mass) moving from x into the region between x_l and x_r,P_e, is defined as:

$$
P_e = \int_{\frac{x_l-x}{\Delta t}}^{\frac{x_r-x}{\Delta t}} \frac{(0.5v_x^2+C)}{\sqrt{2\pi}s}\exp\left(\frac{-(v_x-m)^2}{2s^2}\right)dv_x \tag{23}
$$

where C is the internal energy ($\frac{J}{kg}$) of a molecule and represents the energy stored in it's vibrational and rotational degrees of freedom. The equipartition theory implies that each degree of freedom holds $0.5kT$ joules of energy per particle, or $0.5RT$ joules of energy per kg. Therefore, $C = \frac{1}{2}\zeta RT$, where ζ = number of internal degrees of freedom. The general solution to this integral is:

$$
P_e = \left[\frac{1}{4}\left(m^2+s^2+2C\right)\operatorname{erf}\left(\frac{x-m}{\sqrt{2}s}\right) - \frac{s}{2\sqrt{2\pi}}\exp\left(\frac{-(m-x)^2}{2s^2}\right)\right]_{\frac{x_l-x}{\Delta t}}^{\frac{x_r-x}{\Delta t}} \tag{24}
$$

Substituting the specified bounds gives the result:

$$
\begin{aligned}
&P_e = \tfrac{1}{4}(m^2+s^2+2C)\left[\operatorname{erf}\left(\tfrac{mt+x-x_l}{\sqrt{2}st}\right) - \operatorname{erf}\left(\tfrac{mt+x-x_r}{\sqrt{2}st}\right)\right] \\
&+\tfrac{s}{2t\sqrt{2\pi}}\left[(mt+x_l-x)\exp\left(\tfrac{-(mt+x-x_l)^2}{2s^2t^2}\right) - (mt+x_r-x)\exp\left(\tfrac{-(mt+x-x_r)^2}{2s^2t^2}\right)\right]
\end{aligned}
\tag{25}
$$

The cumulative fraction of energy over the range x_L to x_R to flow into the region between x_l and x_r we will call f_{EE}. This is evaluated as:

$$
f_{EE} = \int_{x_L}^{x_R} P_e dx \tag{26}
$$

The general solution to this integral is:

$$f_{EE} = \frac{1}{4}\left[\begin{array}{l} +\left[(x-x_l)(m^2+s^2+2C)+mt(m^2+3s^2+2C)\right]\mathrm{erf}\left(\frac{mt+x-x_l}{\sqrt{2}st}\right) \\ -\left[(x-x_r)(m^2+s^2+2C)+mt(m^2+3s^2+2C)\right]\mathrm{erf}\left(\frac{mt+x-x_r}{\sqrt{2}st}\right) \\ +\sqrt{\frac{2}{\pi}}st\left(m^2+2s^2+2C\right)\exp\left(\frac{-(mt+x-x_l)^2}{2s^2t^2}\right) \\ -\sqrt{\frac{2}{\pi}}st\left(m^2+2s^2+2C\right)\exp\left(\frac{-(mt+x-x_r)^2}{2s^2t^2}\right) \end{array}\right]_{x_L}^{x_R} \tag{27}$$

Substituting the bounds obtains:

$$\begin{array}{l} f_{EE} = \frac{st\left(m^2+2s^2+2C\right)}{2\sqrt{2\pi}} \\ \left[\exp\left(\frac{-(mt+x_R-x_l)^2}{2s^2t^2}\right)-\exp\left(\frac{-(mt+x_L-x_l)^2}{2s^2t^2}\right)-\exp\left(\frac{-(mt+x_R-x_r)^2}{2s^2t^2}\right)+-\exp\left(\frac{-(mt+x_L-x_r)^2}{2s^2t^2}\right)\right] \\ +\frac{1}{4}\left((x_R-x_l)(m^2+s^2+2C)+mt(m^2+3s^2+2C)\right)\mathrm{erf}\left(\frac{mt+x_R-x_l}{\sqrt{2}st}\right) \\ -\frac{1}{4}\left((x_L-x_l)(m^2+s^2+2C)+mt(m^2+3s^2+2C)\right)\mathrm{erf}\left(\frac{mt+x_L-x_l}{\sqrt{2}st}\right) \\ -\frac{1}{4}\left((x_R-x_r)(m^2+s^2+2C)+mt(m^2+3s^2+2C)\right)\mathrm{erf}\left(\frac{mt+x_R-x_r}{\sqrt{2}st}\right) \\ +\frac{1}{4}\left((x_L-x_r)(m^2+s^2+2C)+mt(m^2+3s^2+2C)\right)\mathrm{erf}\left(\frac{mt+x_L-x_r}{\sqrt{2}st}\right) \end{array} \tag{28}$$

The fluxes that flow into region x_l and x_r where (x_l & $x_r < x_L$) are calculated using similar integrals to the ones above. To calculate the fraction of mass that remains in the region $x_L - x_R$, we use the result from Equation 16 and set $x_l = x_L$ and $x_r = x_R$. The same theory also applies to the momentum and energy fluxes using Equations 22 and 28. The complete set of flux expressions for each region (East, West and Central) can be found in the Appendix.

Figure 2 shows the structured, uniform rectangular mesh to be used for these simulations. To calculate mass flow into the cell directly northeast of cell C (NE), we simply multiply the original mass in cell C by the fraction of the flow in the x direction to land between region x_3 and x_4, and then multiply this amount again by the fraction of the flow in the y direction to land between region y_3 and y_4. This can also be shown by:

$$M_{NE} = f_{ME}.f_{MN}.m_0 \tag{29}$$

Where M_{NE} is the gross flux of mass from cell C to cell NE and m_0 is the original mass (kg) in cell C. Re-substituting $s = \sqrt{RT}$, $m = V_x$, $t = \Delta t$, $x_L = x_2$, $x_R = x_3$,$x_l = x_3$ and $x_r = x_4$, the fraction of the total mass in the cell which flows from the central cell ($x_2 \rightarrow x_3$) into the column $x_3 \rightarrow x_4$ can be rewritten as:

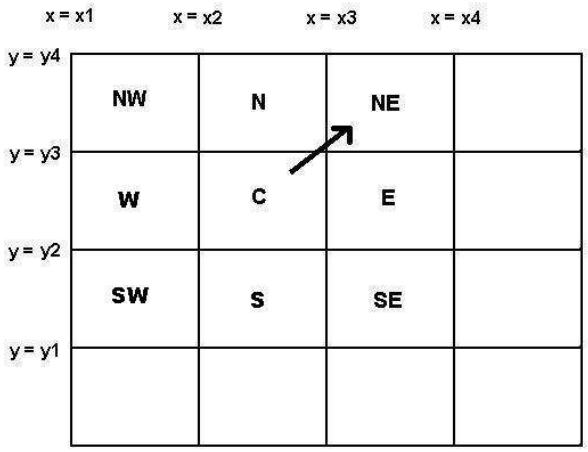

Figure 2: Structured, uniform rectangular mesh used in TDEFM example. Molecules start from a random position within cell C, with a velocity selected from the Maxwell-Boltzmann distribution, and flow (in a small time Δt) to any of the eight contiguous cells labeled NE, N, NW, W, SW, S, SE and E.

$$
\begin{aligned}
f_{ME} &= F\left[\exp(-S_x^2) + \exp\left(-a_{24}^2\right) - \exp\left(-a_{23}^2\right) - \exp\left(-a_{34}^2\right)\right] \\
&+\tfrac{1}{2}\mathrm{erf}\ \left(S_x\right) V_x \Delta t/\Delta z \\
&+\tfrac{1}{2}\mathrm{erf}\ \left(a_{24}\right)\left(V_x\Delta t + x_2 - x_4\right)/\Delta z \\
&-\tfrac{1}{2}\mathrm{erf}\ \left(a_{23}\right)\left(V_x\Delta t + x_2 - x_3\right)/\Delta z \\
&-\tfrac{1}{2}\mathrm{erf}\ \left(a_{34}\right)\left(V_x\Delta t + x_3 - x_4\right)/\Delta z
\end{aligned}
\tag{30}
$$

where the following non-dimensional constants have been defined:

$$
\begin{aligned}
F &= \tfrac{c_m \Delta t}{2\sqrt{\pi}\Delta z} \\
S_x &= V_x/c_m \\
c_m &= \sqrt{2RT} \\
a_{23} &= \left(x_2 - x_3 + V_x\Delta t\right)/c_m\Delta t \\
a_{24} &= \left(x_2 - x_4 + V_x\Delta t\right)/c_m\Delta t \\
a_{34} &= \left(x_3 - x_4 + V_x\Delta t\right)/c_m\Delta t.
\end{aligned}
\tag{31}
$$

Here Δz is the flow field thickness in the z direction which can be taken as unity for 2D flow. Similar expressions can be derived for the other cells, as well as for momentum and energy fluxes. Full flux expressions can be found in the appendix.

Another assumption can be made by keeping the time step Δt very small. By doing so, the chance of particles being able to flow more than the immediately adjacent cell becomes almost zero and instead of calculating the fraction of flow specifically between x_3 and x_4 we can use the EFM equivalent flux by itself. This assumes that all of the flux

that crosses x_3 in any given time step will not cross x_4. With a small enough time step, restricted to one dimension, this approach should equal the TDEFM approach. This faster method, called 'QTDEFM' for *Quick* TDEFM, can be implemented using the ordinary EFM fluxes for a single flow across a surface. The equivalent term for f_{ME}, or the mass fraction to flow across the surface at x_2 to an infinite distance $x_2 + \infty$ is:

$$f_{ME} = \frac{\Delta t}{\Delta x} \left[(D\rho c_m) + (W_p \rho V) \right]; \tag{32}$$

Where:

$$\begin{aligned} c_m &= \sqrt{2RT} \\ W_p &= \tfrac{1}{2} \left(\operatorname{erf} (S_x) + 1 \right) \\ S_x &= \tfrac{V}{c_m} \\ D &= \tfrac{1}{2\sqrt{\pi}} \exp \left(-S_x^2 \right) \\ \rho &= 1 \end{aligned} \quad . \tag{33}$$

Using this method assumes that all of the fluxes that cross x_2 are captured in the cell immediately adjacent to the central cell, while TDEFM only captures the mass that falls into a specific range. Any mass, energy or momentum that is not captured in the regions examined by TDEFM are assumed to be kept by the donor cell. The small fraction of fluxes held by the donor cell can be minimised through manipulation of the time step and cell size. This method is examined in the results section and compared with the full TDEFM solver.

2.1 Numerical Validation of TDEFM Fluxes

Direct simulations run in MATLAB were used to verify the TDEFM fluxes. n simulation particles with unit mass were placed a region of unit volume. The mean velocities m_x and m_y in the central region were set to unity as was the time step. Particles were moved through a single time step, and no particle interactions were allowed to occur. Figure 3 shows the central (shaded) region located between $10 < x < 11$ and $10 < y < 11$. The fractions of mass, energy and momentum were calculated for regions A, C, E and for the general region F, which can exist anywhere in the flow field and does not need to share a common interface with the shaded region for mass, momentum or energy transfer to occur. As the number n of simulation particles increases, the fluxes calculated through direct simulation are expected to rapidly approach the TDEFM fluxes derived. Defining region F by setting $x_1 = 13, x_2 = 14, y_1 = 13$ and $y_2 = 14$, we can simulate a cell diagonally adjacent to the shaded region, although we could have chosen any region in the flow with equally successful results. If the mass flux fraction into region F calculated by TDEFM is f_{MF}^T and the fraction obtained from direct simulation is f_{MF}^S, then $\lim_{n\to\infty} \left(f_{MF}^T - f_{MF}^S \right)$ should equal zero. This can be shown in Table 1. The mean difference and variance between these fluxes are both decreasing as the number of simulated particles increases, implying that the fluxes calculated by TDEFM are correct.

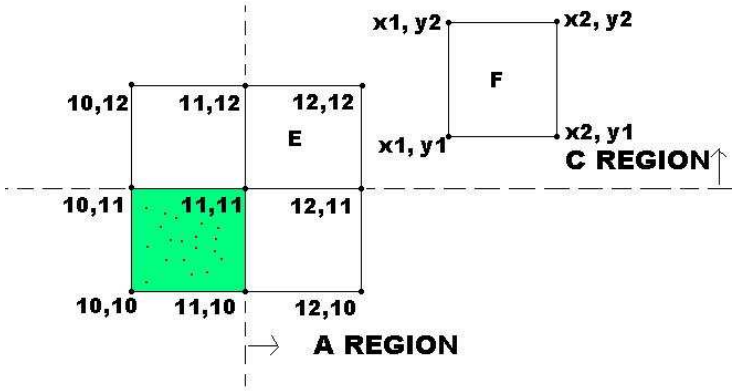

Figure 3: Setup for the numerical validation of the TDEFM fluxes. Region A is defined as the entire region where $x > 11$, while region C is $y > 11$. The bulk velocities in the x and y direction are mx and my respectively. Region E is the cell diagonally adjacent from the central, shaded cell. Region F is located at any point in space defined by x_1, x_2, y_1 and y_2.

n	mean$(f^T_{MF} - f^S_{MF})$	var$(f^T_{MF} - f^S_{MF})$
100	2.985e-3	2.944e-4
1000	4.414e-3	8.493e-5
10,000	7.043e-4	4.392e-6
100,000	1.762e-5	3.374e-7

Table 1: The absolute value of mean difference and the variance of the difference between analytically calculated and directly simulated mass flux fractions. Both the mean and the variance of the difference, defined as $f^T_{MF} - f^S_{MF}$, can be seen to approach zero as the number of simulation particles increases. f^T_{MF} is the mass flux fraction calculated by TDEFM, f^T_{MF} represents the simulated mass flux fraction. Subscript MF represents the mass flux fraction into region F.

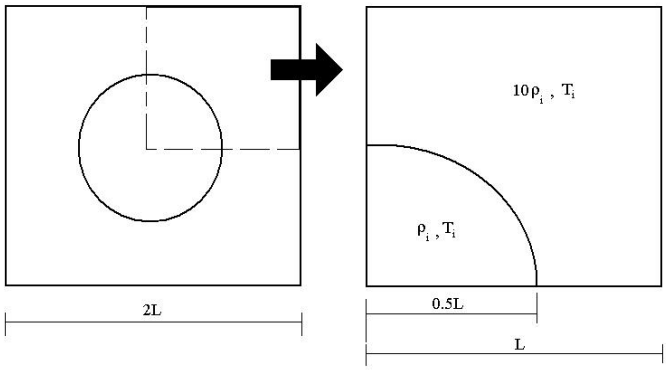

Figure 4: Computational domain for the implosion problem. A circular region of low density gas is surrounded by a high density gas contained in a square region with side $2L$. The origin is at the center of the circle. One quarter the square domain is considered. The symmetry boundary condition (specular reflection) was applied at x and y axes. Perfect gas with ratio of specific heats $\gamma = 5/3$. Initial conditions: $T_H/T_L = 1$, $\rho_H/\rho_L = 10$ (pressure ratio $P_H/P_L = 10$). Radius of low pressure region is $L/2$.

3 Results

The problems associated with direction decoupling can be demonstrated by calculating a 2D imploding shock wave on a rectangular mesh. Figure 4 shows the computational domain and the initial condition in which there is a low pressure cylindrical region surrounded by a high pressure region with a sharp discontinuity between the two. A cylindrically symmetric shock wave will propagate toward the center, causing an increase in temperature and density as the shock travels inwards. The initial low pressure region in the center was a circle located in a square region with a radius of $0.5L$, where $2L$ is the length of the square region. There was no temperature ratio between the high and low pressure regions, and the density ratio was 10. The flow was run just prior to the imploding shock reflecting at the origin. Symmetry has been exploited and so only the flow of the 'North Eastern' section was considered. Simulations of the entire region show that this is reasonable. The flow is assumed inviscid, no heat transfer is present and the gas is assumed ideal. For simplicity the results presented are for simple monoatomic molecules where the molecules have energy of translation only, *i.e.* no rotational, vibrational, ionization or chemical potential energy and the ratio of specific heats $\gamma = 5/3$.

Presented are the results of a simple 2D implosion problem obtained from the TDEFM, EFM and Riemann solver used. The QTDEFM and TDEFM methods are also compared. The outer boundaries are reflective boundaries. Both 1st and 2nd order in time solutions were considered, as were 1st and 2nd order in space solutions for the Riemann solver.

Figure 5 shows a contour plot of density taken from TDEFM. It can be seen that the contours are generally round and symmetric as is expected. Figure 6 gives the contours of density from direction decoupled EFM. The contours shown are not round, and are skewed along the diagonal. Figure 7 is a contour of density from an approximate Riemann solver, and shows the same skewing occurs as shown in figure 6. This asymetric

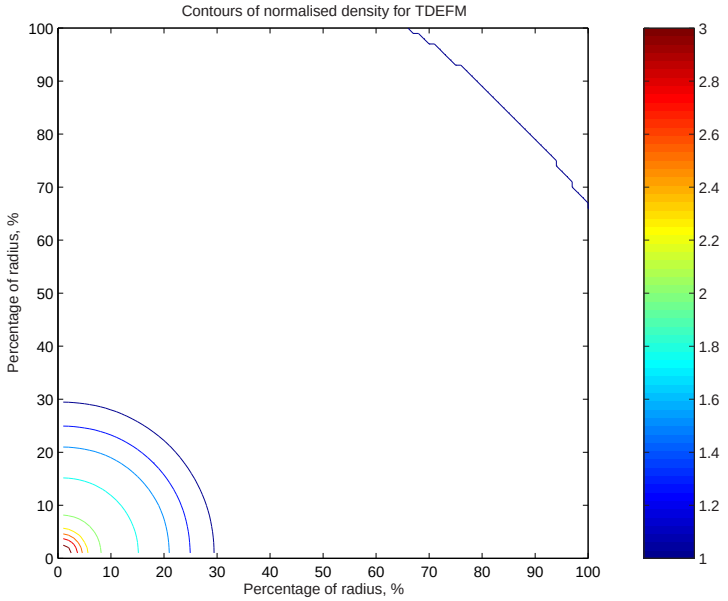

Figure 5: Contours of normalized density versus radial position for TDEFM. $\frac{T_H}{T_L} = 1$, $\frac{\rho_H}{\rho_L} = 10$. Simulation run for 100 time steps of $\frac{a}{L}\Delta t = 0.000348$. The speed of sound is $a = \sqrt{\gamma RT}$. Each contour represents an increase/decrease of 0.25.

behaviour, or skewing, demonstrates the weakness of the EFM and Riemann solver. The amount of skewing can be affected by the number of cells used, however, regardless of the cell density TDEFM still shows more symmetric results. This skewing can also be removed by the implementation of 2nd order in time or space methods, both of which are more computationally expensive than the 1st order TDEFM. However, implementation of increased order in time simulations show that TDEFM remains superior.

Figure 8 shows a graph of density *vs.* radial position comparing the various solvers. It can be seen that along the x axis the results are in general agreement. Since the effect of the addition of diagonal fluxes is not present along this line, the EFM and TDEFM solutions agree very closely. The approximate Riemann solver used also keeps in good agreement with the TDEFM and EFM solutions. Likewise, the graph of temperature vs radial position in Figure 9 shows the results are in general agreement. All of the features expected in the imploding shock are present, as in Figure 8.

Figure 10 is a graph showing the local variance of temperature as a function of radius. The local variance of temperature was calculated using the following process:

1. For each cell, calculate the distance R from the cell center to the imploding region center.
2. Sort each cell and its temperature by radius R.
3. For a given region ΔR, calculate the local variance and mean of the temperature.
4. Normalize the local variance by the local mean temperature.
5. Progress along R from R = 0 in steps of ΔR up to R.

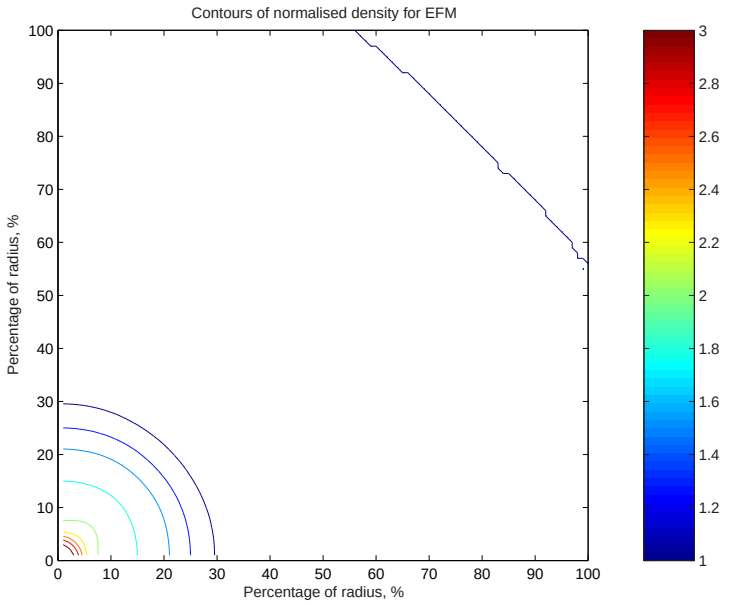

Figure 6: Contours of normalised density versus radial position for EFM. $\frac{T_H}{T_L} = 1$, $\frac{\rho_H}{\rho_L} = 10$. Simulation run for 100 time steps of $\frac{a}{L}\Delta t = 0.002955$. Each contour represents an increase/decrease of 0.25.

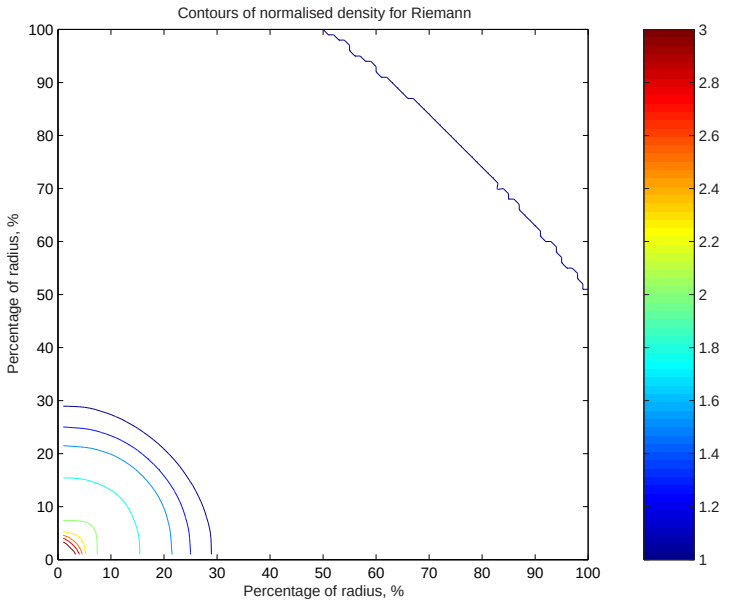

Figure 7: Contours of normalized density versus radial position for Riemann. $\frac{T_H}{T_L} = 1$, $\frac{\rho_H}{\rho_L} = 10$. Simulation run for 100 time steps of $\frac{a}{L}\Delta t = 0.002955$. Each contour represents an increase/decrease of 0.25.

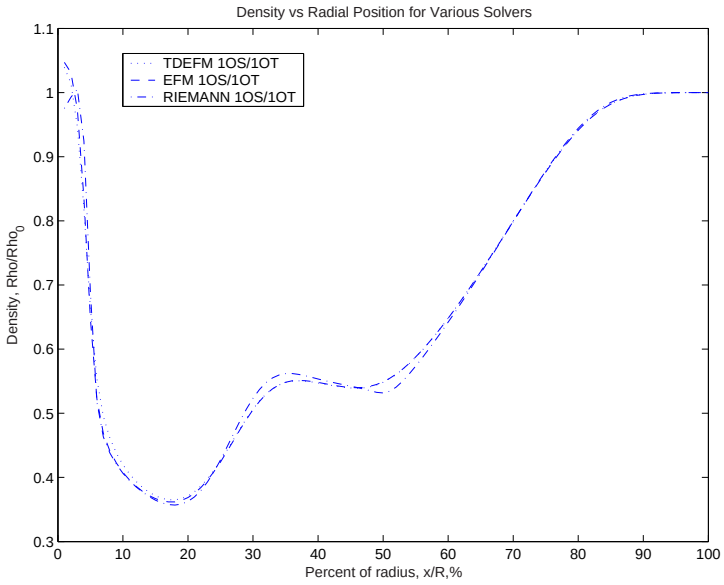

Figure 8: Plots of normalized density versus radial position along the x axis. 1OS = 1st order in space, 1OT = 1st order in time. $\frac{T_H}{T_L} = 1$, $\frac{\rho_H}{\rho_L} = 10$. Simulation run for 100 time steps of $\frac{a}{La}\Delta t = 0.002955$. Reflection at the origin has not yet occurred. Density is normalised by the initial density in the low pressure region.

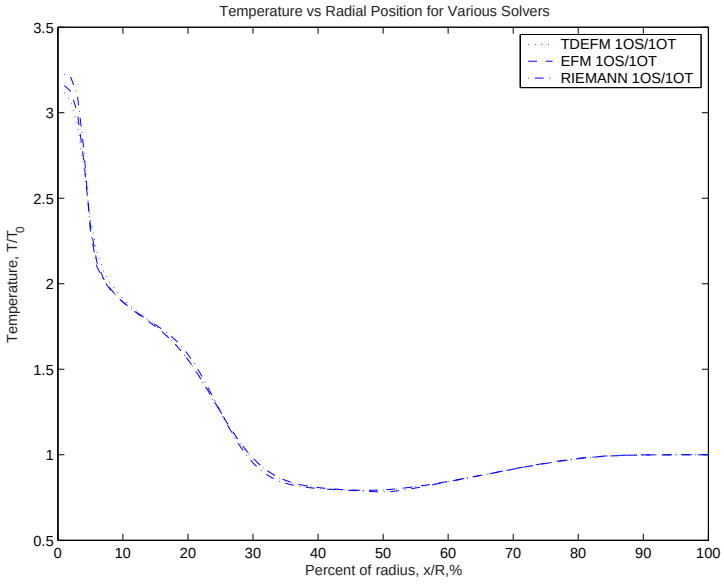

Figure 9: Plots of normalized temperature versus radial position along the x axis. 1OS = 1st order in space, 1OT = 1st order in time. $\frac{T_H}{T_L} = 1$, $\frac{\rho_H}{\rho_L} = 10$. Simulation run for 100 time steps of $\frac{a}{L}\Delta t = 0.000348$. Temperature is normalised by the original temperature in the low pressure region.

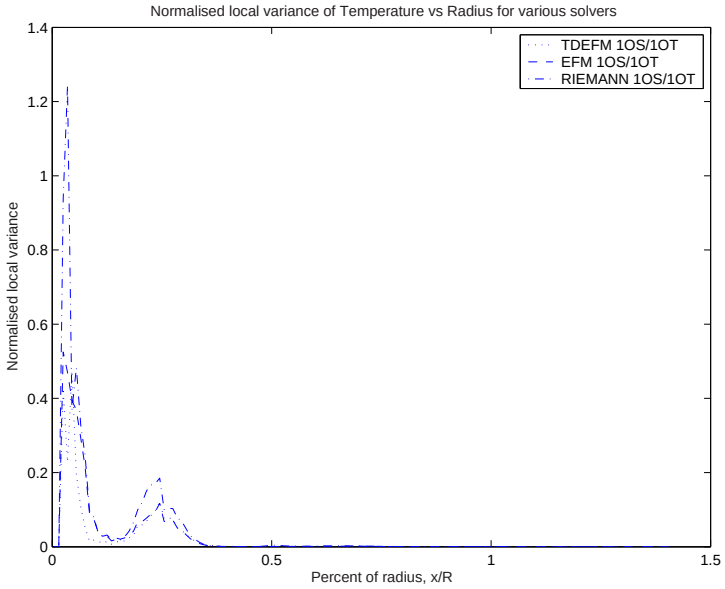

Figure 10: Plots of normalized variance in local temperature versus radial position along the x axis. 1OS = 1st order in space, 1OT = 1st order in time. $\frac{T_H}{T_L} = 1$, $\frac{\rho_H}{\rho_L} = 10$. Simulation run for 100 time steps of $\frac{a}{L}\Delta t = 0.000348$. The variance in temperature was normalised using the local mean temperature.

For any given radius, the value of temperature should be identical. However, with the skewing that is apparent in Figures 6 and 7 the temperatures can vary quite significantly. With a finer mesh and a correspondingly higher number of points, the variance will be reduced. However, it has been found that the relative variance between the different solvers shows the same trends.

Figure 11 shows a plot of normalised local variance of temperature vs normalised distance from the origin when $\Delta y = \frac{2}{3}\Delta x$. This variance is generally increased from the previous examples where cells were square in shape rather than rectangular, implying that rectangular cells lead to higher errors in such flows. Regardless of this change in cell shape, TDEFM still shows more symmetrical results than the EFM or Riemann solvers. The comparison between the derived TDEFM and QTDEFM methods can be seen in Figure 12. The difference in temperature is almost indistinguishable on a plot, however, the difference can be seen when examining the normalised local variance of temperature. The scale of this difference is so slight - on the order of 2.5 percent of the maximum local normalised variance - that one can comfortably use QTDEFM when an increase in computational speed is desired without a significant loss of accuracy.

4 Conclusion

The implementation of TDEFM on a structured, uniform rectangular mesh has been investigated and compared to other solvers. TDEFM is a kinetic theory based flux method derived through integration of velocities and location rather than fluxes across a surface. Therefore, TDEFM can calculate mass, energy and momentum fluxes to any region in

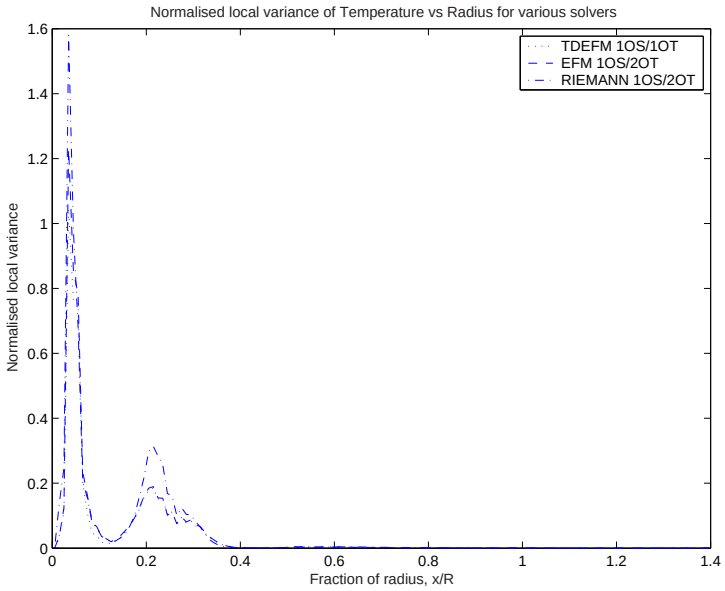

Figure 11: Plots of normalized variance in local temperature versus radial position along the x axis when $\Delta y = \frac{2}{3}\Delta x$. 1OS = 1st order in space, 1OT = 1st order in time. $\frac{T_H}{T_L} = 1$, $\frac{\rho_H}{\rho_L} = 10$. Simulation run for 100 time steps of $\frac{a}{L}\Delta t = 0.000348$. The variance in temperature was normalised using the local mean temperature.

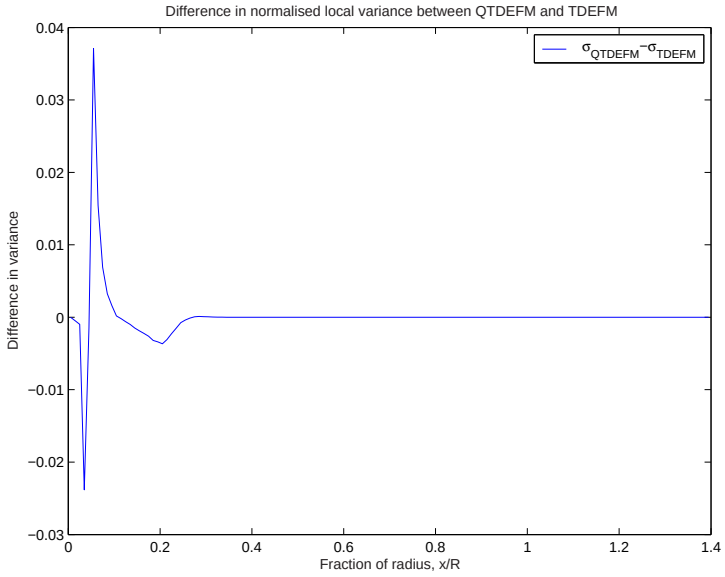

Figure 12: A plot of the difference in the normalised local variance versus radial position for QTDEFM and TDEFM along the x axis when $\Delta y = \frac{2}{3}\Delta x$. 1OS = 1st order in space, 1OT = 1st order in time. $\frac{T_H}{T_L} = 1$, $\frac{\rho_H}{\rho_L} = 10$. Simulation run for 100 time steps of $\frac{a}{L}\Delta t = 0.000348$. The variance in temperature was normalised using the local mean temperature.

the flow from a given starting cell. In its simplified form, TDEFM fluxes are not only exchanged between directly adjacent cells but also diagonally adjacent cells. In its full form, as provided in the derivation, TDEFM provides the fluxes from any starting region to any other region in the flow. The method was tested in two dimensions by simulating an imploding shock.
Simulations have been restricted to 1st order in space and up to 2nd order in time. Results show that on a structured, uniform rectangular mesh TDEFM and QTDEFM can capture un-aligned flows with greater accuracy than the direction split methods.

Future potential exists for the development of TDEFM in higher orders in space, thus further increasing the accuracy of the model. TDEFM can easily be extended into 3D simulations. A faster version of TDEFM, named QTDEFM, has been shown to be nearly as accurate while taking no more than 15 percent longer than direction split EFM and 1 percent less than Riemann. Future applications of the method may include simulations around arbitrary geometries without the use of specialized flow aligned grids or higher order methods.

References

[1] Pullin, D.I., 'Direct Simulation Methods for Compressible Ideal Gas Flow',*J. Comput. Phys.* **34**: 231-244, 1980.

[2] Macrossan, M.N., 'The equilibrium flux method for the calculation of flows with non-equilibrium chemical reactions', *J. Comput. Phys.* **80**: 204-231, 1989.

[3] Macrossan, M.N. and Pullin, D.I., 'A Computational Investigation of Inviscid Hypervelocity Flow of a Dissociating Gas Past a Cone at Incidence', *J. Fluid Mech.* **266**: 69-92, 1994.

[4] Macrossan, M.N., 'Hypervelocity flow of dissociating nitrogen downstream of a blunt nose', *J. Fluid Mech.* **207**: 167-202, 1990.

[5] Lengrand, J.C., Raffin, M. and Allegre, J., *Monte Carlo Simulation Method Applied to Jet Wall Interactions under Continuum Flow Conditions*, in Rarefied Gas Dynamics, edited by S.S Fisher, Prog. Astro. Aero. V.74, AIAA, New York, 994-1006, 1981.od Applied to Jet Wall Interactions under Continuum Flow Conditions, in Rarefied Gas Dynamics, editied by S.S Fisher, Prog. Astro. Aero. V.74, AIAA, New York, 994-1006, 1981.

[6] Cook, G., *High Accuracy Capture of Curved Shock Fronts Using the Method of Space-Time Conservation Element and Solution Element*, 37th AIAA (American Institute of Aeronautics and Astronautics) Aerospace Sciences Meeting and Exhibit, 1998.

[7] Macrossan, M.N., Metchnik, M. and Pinto, P.A., 'Hypersonic flow over a wedge with a particle flux method', In Capetilli, Mario, Eds., *24th International Symposium on Rarefied Gas Dynamics*, **762**: 650-656, 10-16th July, 2004.

[8] Mallett, E.R. and Pullin. D.I. and Macrossan, M.N.,'Numerical study of hpersonic leeward flow over a blunt nosed delta wing',*AIAA J.* **33**: 1626-1633, 1995.

[9] Jacobs, P.A., *MBCNS: A computer program for the simulation of transient compressible flows*, 1998 Update, Department of Mechanical Engineering Report 7/98, The University of Queensland, June 1998.

5 Appendix

5.1 Equilibrium Flux Method

The Equilibrium Flux Method was introduced by Pullin [1] as a solution method for the Euler equations. The fluxes are derived from kinetic theory by assuming an equilibrium distribution of molecular velocities in each computational cell. The fluxes may be formally derived from the Boltzmann equation, but here we derive the fluxes as those which result from the Equilibrium Particle Simulation method, in the limit of an infinite number of particles in each cell, no gradients of density within the cells, and small time δt.

Consider a typical cell surface S with unit normals $\hat{n}$,$\hat{p}$ and $\hat{q}$ attached to the surface. Since the conditions on either side of the surface may be different, the fluxes can be separated into two parts, f^+ and f^-, corresponding to the flow of molecules across the surface in the positive and negative f-direction. Let the velocity of a molecule be denoted by $\vec{v}$, with components $v_n = \vec{v}.\hat{n}$, $v_p = \vec{v}.\hat{p}$, and $v_q = \vec{v}.\hat{q}$. Let:

$$Q = \left[m,\ mv_n,\ mv_p,\ mv_q,\ m\left(\frac{1}{2}\vec{v}.\vec{v} + e_{st}\right)\right] \tag{34}$$

Note that $\frac{1}{2}\vec{v}.\vec{v}$ is the specific translational energy of the molecule and est is the specific energy of molecular structure, such as rotational, vibrational or electronic energy.
The flux of Q across the surface may be evaluated if the distribution functions for molecular velocities on either side of the surface, $g^+ = n_L f_L$ and $g^- = n_R f_R$, are known. Here, n is the number density and $f(\vec{v}, e_{st})d\vec{v}de_{st}$ gives the fraction of molecules with velocity in the range and energy of molecular structure in the range . The subscript L and R denote conditions on the left and right of the surface respectively; $\hat{n}$ points from left to right. The net flux is:

$$F_Q = F_Q^+ + F_Q^- \tag{35}$$

Here:

$$F_Q^+ = \int_0^\infty \int_{-\infty}^\infty \int_{-\infty}^\infty \int_\infty^0 Q_g^+ v_n dv_n dv_p dv_q de_{st} \tag{36}$$

is the flux arising from molecules traveling from the left of the surface to the right. The flux arising from molecules traveling from the right side to the left side is:

$$F_Q^- = \int_0^\infty \int_{-\infty}^\infty \int_{-\infty}^\infty \int_\infty^0 Q_g^- v_n dv_n dv_p dv_q de_{st} \tag{37}$$

If the molecular velocities on either side take on the equilibrium distribution, Equation (36) can be evaluated as:

$$F_Q^+ = W_L \begin{bmatrix} \rho v_n \\ \rho v_n v_n + \rho RT \\ \rho v_n v_p \\ \rho v_n v_q \\ \rho v_n \left(\frac{1}{2}\vec{v}.\vec{v} + C_p T\right) \end{bmatrix} + D_L \begin{bmatrix} \rho c_m \\ \rho c_m v_n \\ \rho c_m v_p \\ \rho c_m v_q \\ \rho c_m \left(\frac{1}{2}\vec{v}.\vec{v} + \frac{1}{2}(\gamma+1)C_v T\right) \end{bmatrix} \tag{38}$$

i.e.

$$\begin{aligned} W_L &= \tfrac{1}{2}\left[1 + \text{erf }(S_n)\right]_L \\ D_L &= \tfrac{1}{2\sqrt{\pi}} \exp\left(-S_n^2\right)_L \\ S_n &= \left(v_n/c_m\right)_L \\ c_m &= \sqrt{2RT}_L \end{aligned} \tag{39}$$

C_p and C_v are the specific heats at constant pressure and volume respectively, and $\gamma = \frac{C_p}{C_v}$. Equivalently, Equation (37) can be evaluated as:

$$F_Q^- = W_R \begin{bmatrix} \rho v_n \\ \rho v_n v_n + \rho RT \\ \rho v_n v_p \\ \rho v_n v_q \\ \rho v_n \left(\frac{1}{2}\vec{v}.\vec{v} + C_p T\right) \end{bmatrix} + D_R \begin{bmatrix} \rho c_m \\ \rho c_m v_n \\ \rho c_m v_p \\ \rho c_m v_q \\ \rho c_m \left(\frac{1}{2}\vec{v}.\vec{v} + \frac{1}{2}(\gamma+1)C_v T\right) \end{bmatrix} \tag{40}$$

I.e

$$\begin{aligned} W_R &= \tfrac{1}{2}\left[1 - \text{erf }(S_n)\right]_R \\ D_R &= -\tfrac{1}{2\sqrt{\pi}} \exp\left(-S_n^2\right)_R \\ S_n &= \left(v_n/c_m\right)_R \\ c_m &= \sqrt{2RT}_R \end{aligned} \tag{41}$$

5.2 TDEFM Flux Expressions

Presented are the mass, energy and momentum equations for fractions of flow in direction x, where x is any global coordinate. Using Equations 16, 22 and 28 and using figure 2 as a general guide the fluxes can be evaluated. The central region C is our donor cell, thus $x_L = x_2$ and $x_R = x_3$. The eastern flux, designated with subscript E, is calculated by setting $x_l = x_R = x_3$ and $x_r = x_4$. Making these substitutions obtains the mass flux per unit mass f_{ME} to flow into the column between x_3 and x_4, which simplifies to:

$$
\begin{aligned}
f_{ME} &= F\left[\exp(-S_x^2) + \exp\left(-a_{24}^2\right) - \exp\left(-a_{23}^2\right) - \exp\left(-a_{34}^2\right)\right] \\
&+\tfrac{1}{2}\text{erf}\ \left(S_x\right) V_x \Delta t/\Delta z \\
&+\tfrac{1}{2}\text{erf}\ \left(a_{24}\right)\left(V_x\Delta t + x_2 - x_4\right)/\Delta z \\
&-\tfrac{1}{2}\text{erf}\ \left(a_{23}\right)\left(V_x\Delta t + x_2 - x_3\right)/\Delta z \\
&-\tfrac{1}{2}\text{erf}\ \left(a_{34}\right)\left(V_x\Delta t + x_3 - x_4\right)/\Delta z
\end{aligned}
\tag{42}
$$

The mass flux per unit mass f_{MC} to remain in the column between x_2 and x_3, designated by subscript C, is calculated by setting $x_L = x_2$ and $x_R = x_3$. This can be evaluated as:

$$
\begin{aligned}
f_{MC} &= F\left[-2\exp(-S_x^2) + \exp\left(-a_{23}^2\right) + \exp\left(-a_{32}^2\right)\right] \\
&-\text{erf}\ \left(S_x\right) V_x \Delta t/\Delta z \\
&+\tfrac{1}{2}\text{erf}\ \left(a_{23}\right)\left(V_x\Delta t + x_2 - x_3\right)/\Delta z \\
&+\tfrac{1}{2}\text{erf}\ \left(a_{32}\right)\left(V_x\Delta t + x_3 - x_2\right)/\Delta z
\end{aligned}
\tag{43}
$$

The western flux, designated by subscript W, is the mass flux per unit mass f_{MC} to flow into the column between x_1 and x_2. This is obtained by substituting $x_l = x_1$, $x_r = x_L = x_2$ and $x_R = x_3$, which evaluates to:

$$
\begin{aligned}
f_{MW} &= F\left[\exp(-S_x^2) - \exp\left(-a_{21}^2\right) + \exp\left(-a_{31}^2\right) - \exp\left(-a_{32}^2\right)\right] \\
&+\tfrac{1}{2}\text{erf}\ \left(S_x\right) V_x \Delta t/\Delta z \\
&-\tfrac{1}{2}\text{erf}\ \left(a_{21}\right)\left(V_x\Delta t + x_2 - x_1\right)/\Delta z \\
&+\tfrac{1}{2}\text{erf}\ \left(a_{31}\right)\left(V_x\Delta t + x_3 - x_1\right)/\Delta z \\
&-\tfrac{1}{2}\text{erf}\ \left(a_{32}\right)\left(V_x\Delta t + x_3 - x_2\right)/\Delta z
\end{aligned}
\tag{44}
$$

The momentum flux per unit mass f_{PE} from cell C that crosses into the column between x_3 and x_4 is calculated making the same substitutions for x_l, x_r, x_R and x_L as the eastern mass flux. Rearranging Equation 22 and making these substitutions gives:

$$
\begin{aligned}
f_{PE} &= FV_x\left[\exp(-S_x^2) + \exp\left(-a_{24}^2\right) - \exp\left(-a_{23}^2\right) - exp\left(-a_{34}^2\right)\right] \\
&+\tfrac{1}{2}\text{erf }\left(S_x\right)\left[(V_x^2 + \tfrac{1}{2}c_m^2)\Delta t\right]/\Delta z \\
&+\tfrac{1}{2}\text{erf }\left(a_{24}\right)\left[(V_x^2 + \tfrac{1}{2}c_m^2)\Delta t + (x_2 - x_4)V_x\right]/\Delta z \\
&-\tfrac{1}{2}\text{erf }\left(a_{23}\right)\left[(V_x^2 + \tfrac{1}{2}c_m^2)\Delta t + (x_2 - x_3)V_x\right]/\Delta z \\
&-\tfrac{1}{2}\text{erf }\left(a_{34}\right)\left[(V_x^2 + \tfrac{1}{2}c_m^2)\Delta t + (x_3 - x_4)V_x\right]/\Delta z
\end{aligned}
\tag{45}
$$

The momentum flux per unit mass f_{PC} from cell C to remain in the column between x_2 and x_3 is:

$$
\begin{aligned}
f_{PC} &= FV_x\left[-2\exp(-S_x^2) + \exp\left(-a_{23}^2\right) + \exp\left(-a_{32}^2\right)\right] \\
&-\text{erf }\left(S_x\right)\left[(V_x^2 + \tfrac{1}{2}c_m^2)\Delta t\right]/\Delta z \\
&+\tfrac{1}{2}\text{erf }\left(a_{23}\right)\left[(V_x^2 + \tfrac{1}{2}c_m^2)\Delta t + (x_2 - x_3)V_x\right]/\Delta z \\
&+\tfrac{1}{2}\text{erf }\left(a_{32}\right)\left[(V_x^2 + \tfrac{1}{2}c_m^2)\Delta t + (x_3 - x_2)V_x\right]/\Delta z
\end{aligned}
\tag{46}
$$

The momentum flux per unit mass f_{PW} from cell C that crosses into the column between x_1 and x_2 is:

$$
\begin{aligned}
f_{PW} &= FV_x\left[\exp(-S_x^2) - \exp\left(-a_{21}^2\right) + \exp\left(-a_{31}^2\right) - exp\left(-a_{32}^2\right)\right] \\
&+\tfrac{1}{2}\text{erf }\left(S_x\right)\left[(V_x^2 + \tfrac{1}{2}c_m^2)\Delta t\right]/\Delta z \\
&-\tfrac{1}{2}\text{erf }\left(a_{21}\right)\left[(V_x^2 + \tfrac{1}{2}c_m^2)\Delta t + (x_2 - x_1)V_x\right]/\Delta z \\
&+\tfrac{1}{2}\text{erf }\left(a_{31}\right)\left[(V_x^2 + \tfrac{1}{2}c_m^2)\Delta t + (x_3 - x_1)V_x\right]/\Delta z \\
&-\tfrac{1}{2}\text{erf }\left(a_{32}\right)\left[(V_x^2 + \tfrac{1}{2}c_m^2)\Delta t + (x_3 - x_2)V_x\right]/\Delta z
\end{aligned}
\tag{47}
$$

The energy flux per unit mass f_{EE} from cell C that crosses into the column between x_3 and x_4 is:

$$
\begin{aligned}
&f_{EE} = [(1/2)(V_x^2 + C_m^2 + 2C)]\, F\, [\exp(-S_x^2) + \exp(-a_{24}^2) - \exp(-a_{23}^2) - exp(-a_{34}^2)] \\
&+\tfrac{1}{4}\text{erf}\ (S_x)\, (V_x^2 + \tfrac{3}{2}C_m^2 + 2C)V_x\Delta t/\Delta z \\
&+\tfrac{1}{4}\text{erf}\ (a_{24}) \left[(V_x^2 + \tfrac{3}{2}C_m^2 + 2C)V_x\Delta t + (x_2 - x_4)(V_x^2 + \tfrac{1}{2}c_m^2)\right]/\Delta z \\
&+\tfrac{1}{4}\text{erf}\ (a_{23}) \left[(V_x^2 + \tfrac{3}{2}C_m^2 + 2C)V_x\Delta t + (x_2 - x_3)(V_x^2 + \tfrac{1}{2}c_m^2)\right]/\Delta z \\
&+\tfrac{1}{4}\text{erf}\ (a_{34}) \left[(V_x^2 + \tfrac{3}{2}C_m^2 + 2C)V_x\Delta t + (x_3 - x_4)(V_x^2 + \tfrac{1}{2}c_m^2)\right]/\Delta z
\end{aligned}
\tag{48}
$$

The energy flux per unit mass f_{EC} from cell C that remains in the column between x_2 and x_3 is:

$$
\begin{aligned}
&f_{EC} = [(1/2)(V_x^2 + C_m^2 + 2C)]\, F\, [-2\exp(-S_x^2) + \exp(-a_{32}^2) - \exp(-a_{23}^2)] \\
&-\tfrac{1}{2}\text{erf}\ (S_x)\, (V_x^2 + \tfrac{3}{2}C_m^2 + 2C)V_x\Delta t/\Delta z \\
&+\tfrac{1}{4}\text{erf}\ (a_{32}) \left[(V_x^2 + \tfrac{3}{2}C_m^2 + 2C)V_x\Delta t + (x_3 - x_2)(V_x^2 + \tfrac{1}{2}c_m^2)\right]/\Delta z \\
&+\tfrac{1}{4}\text{erf}\ (a_{23}) \left[(V_x^2 + \tfrac{3}{2}C_m^2 + 2C)V_x\Delta t + (x_2 - x_3)(V_x^2 + \tfrac{1}{2}c_m^2)\right]/\Delta z
\end{aligned}
\tag{49}
$$

The energy flux per unit mass f_{EW} from cell C that crosses into the column between x_1 and x_2 is:

$$
\begin{aligned}
&f_{EE} = [(1/2)(V_x^2 + C_m^2 + 2C)]\, F\, [\exp(-S_x^2) + \exp(-a_{21}^2) - \exp(-a_{31}^2) - exp(-a_{32}^2)] \\
&+\tfrac{1}{4}\text{erf}\ (S_x)\, (V_x^2 + \tfrac{3}{2}C_m^2 + 2C)V_x\Delta t/\Delta z \\
&+\tfrac{1}{4}\text{erf}\ (a_{21}) \left[(V_x^2 + \tfrac{3}{2}C_m^2 + 2C)V_x\Delta t + (x_2 - x_1)(V_x^2 + \tfrac{1}{2}c_m^2)\right]/\Delta z \\
&-\tfrac{1}{4}\text{erf}\ (a_{31}) \left[(V_x^2 + \tfrac{3}{2}C_m^2 + 2C)V_x\Delta t + (x_3 - x_1)(V_x^2 + \tfrac{1}{2}c_m^2)\right]/\Delta z \\
&-\tfrac{1}{4}\text{erf}\ (a_{32}) \left[(V_x^2 + \tfrac{3}{2}C_m^2 + 2C)V_x\Delta t + (x_3 - x_2)(V_x^2 + \tfrac{1}{2}c_m^2)\right]/\Delta z
\end{aligned}
\tag{50}
$$

Where:

$$
\begin{aligned}
S_y &= V_y/c_m \\
c_m &= \sqrt{2RT} \\
a_{21} &= (x_2 - x_1 + V_x\Delta t)/c_m\Delta t \\
a_{23} &= (x_2 - x_3 + V_x\Delta t)/c_m\Delta t \\
a_{24} &= (x_2 - x_4 + V_x\Delta t)/c_m\Delta t \\
a_{31} &= (x_3 - x_1 + V_x\Delta t)/c_m\Delta t \\
a_{32} &= (x_3 - x_2 + V_x\Delta t)/c_m\Delta t \\
a_{34} &= (x_3 - x_4 + V_x\Delta t)/c_m\Delta t
\end{aligned}
\tag{51}
$$

and Δz is the flow field thickness in the z direction which can be taken as unity for 2D flow. C represents the energy stored in each molecules vibrational and rotational energy. (J/kg) These equations can be multiplied together to obtain fluxes into all cells shown in figure 2.